

ASEHybrid: When Geometry Matters Beyond Homophily in Graph Neural Networks

Shalima Binta Manir¹ Tim Oates¹

Abstract

Standard message-passing graph neural networks (GNNs) often struggle on graphs with low homophily, yet homophily alone does not explain this behavior, as graphs with similar homophily levels can exhibit markedly different performance and some heterophilous graphs remain easy for vanilla GCNs. Recent work suggests that *label informativeness* (LI), the mutual information between labels of adjacent nodes, provides a more faithful characterization of when graph structure is useful. In this work, we develop a unified theoretical framework that connects curvature-guided rewiring and positional geometry through the lens of label informativeness, and instantiate it in a practical geometry-aware architecture, *ASEHybrid*. Our analysis provides a *necessary-and-sufficient* characterization of when geometry-aware GNNs can improve over feature-only baselines: such gains are possible if and only if graph structure carries label-relevant information beyond node features. Theoretically, we relate adjusted homophily and label informativeness to the spectral behavior of label signals under Laplacian smoothing, show that degree-based Forman curvature does not increase expressivity beyond the one-dimensional Weisfeiler-Lehman test but instead reshapes information flow, and establish convergence and Lipschitz stability guarantees for a curvature-guided rewiring process. Empirically, we instantiate ASEHybrid using Forman curvature and Laplacian positional encodings and conduct controlled ablations on CHAMELEON, SQUIRREL, TEXAS, TOLOKERS, and MINESWEEPER, observing gains precisely on label-informative heterophilous benchmarks where graph structure provides label-relevant information beyond node features, and no meaning-

ful improvement in high-baseline regimes.

1. Introduction

Graph neural networks (GNNs) implement a message-passing paradigm in which node representations are iteratively updated by aggregating information from their neighbors (Scarselli et al., 2008; Gilmer et al., 2017). This mechanism underlies many successful architectures and performs particularly well on graphs with *homophilous* structure, where adjacent nodes tend to share labels (Kipf & Welling, 2017). However, on *heterophilous* graphs where neighbors often belong to different classes—standard GNNs can fail dramatically, and in some cases simple feature-only classifiers match or outperform graph-based models (Zhu et al., 2020; Platonov et al., 2023).

The degree of homophily by itself is insufficient to characterize when message passing helps. Different homophily definitions can disagree sharply and are not directly comparable across datasets with varying class counts or imbalance (Zhu et al., 2020). Moreover, there exist heterophilous graphs on which vanilla GCNs perform well, as well as graphs with similar homophily levels but markedly different GNN performance (Ma et al., 2022). To address these limitations, recent work has proposed *adjusted homophily* and *label informativeness* (LI) as more principled structural descriptors (Platonov et al., 2023). LI captures how informative a neighbor’s label is about a node’s label, and empirically correlates more strongly with GNN performance than homophily alone. Platonov et al. (Platonov et al., 2023) view label informativeness as an intrinsic property of the data distribution. We build on this insight by adopting a model-level perspective, characterizing when graph structure can be exploited by learning architectures via the conditional mutual information $I(Y; E | X)$, which quantifies how much label-relevant information about Y the graph structure E contains beyond node features X , and analyzing how curvature-based signals, positional encodings, and rewiring operationalize (or fail to operationalize) this information. Our model is designed for settings in which graph structure provides label-relevant information beyond node features, rather than for feature-dominated regimes. Since homophily alone does not determine whether edges are informative in

¹Department of Computer Science, University of Maryland, Baltimore County, USA. Correspondence to: Shalima Binta Manir <smanir1@umbc.edu>, Tim Oates <oates@cs.umbc.edu>.

this sense, our analysis and experiments focus on datasets where label informativeness, rather than homophily, is the primary explanatory factor.

In parallel, there has been growing interest in *geometric augmentations* for GNNs, including structural encodings, positional encodings, and graph rewiring. Local Curvature Profiles (LCP), based on discrete Ricci curvature, provide node-level summaries of local graph geometry and have been shown to improve performance, especially when combined with Laplacian positional encodings (LapPE) (Fesser & Weber, 2024; Dwivedi & Bresson, 2020). Curvature-guided rewiring modifies the graph structure by adding edges to mitigate over-squashing (Topping et al., 2022).

While recent work has explored combining structural and positional encodings (Fesser & Weber, 2024), integrating curvature-based encodings with curvature-guided rewiring to jointly influence both representations and topology remains unexplored. In contrast, our proposed model, *ASE-Hybrid*, integrates node-level structural encodings (LCP), global positional encodings (LapPE), edge-level curvature conditioning, and curvature-guided rewiring within a single architecture, allowing geometric information to jointly shape feature representations and message passing.

This variability raises several fundamental questions:

- **When should curvature and positional geometry help?**
- **What is the role of homophily and label informativeness?**
- **Can curvature-guided rewiring be formalized?**

In this work, we address these questions by developing a unified theoretical framework that connects curvature-guided rewiring and positional geometry from the perspective of label informativeness, and by grounding the analysis in carefully controlled experiments on heterophilous benchmarks.

1.1. Our Contributions

(A) Structural characterization via adjusted homophily and label informativeness We adopt adjusted homophily and label informativeness (LI) as the primary structural descriptors of node-classification graphs (Platonov et al., 2023). Within this framework:

- We relate adjusted homophily to the spectral concentration of label signals under Laplacian smoothing, explaining why standard GCNs are biased toward low-frequency, homophilous label structure.
- We show that LI naturally arises in an information-theoretic comparison between models that can exploit

graph edges and those restricted to node features (and positional encodings), yielding a condition of the form $I(Y; E | X) > 0$ under which access to edges strictly reduces Bayes risk.

(B) Curvature-weighted diffusion and expressivity We formalize Forman curvature as a local, degree-based edge attribute (Forman, 2003; Sreejith et al., 2016) and analyze its role in message passing:

- We show that incorporating Forman curvature as a local edge feature does *not* increase expressive power beyond the one-dimensional Weisfeiler–Lehman (1-WL) test, as standard message-passing GNNs are at most as powerful as 1-WL in distinguishing graph structures (Xu et al., 2019).
- In contrast, we show that non-local edge attributes and sufficiently rich positional encodings can strictly increase the distinguishing power of GNNs over plain 1-WL.

(C) Curvature-guided rewiring: convergence and stability We study a simple curvature-guided rewiring process inspired by discrete geometric flows (Topping et al., 2022). We prove finite termination and convergence under a Lyapunov-style objective based on curvature regularization, and establish Lipschitz stability with respect to bounded edge-edit perturbations.

(D) ASEHybrid: a practical geometry-aware architecture We instantiate the framework in *ASEHybrid*, a geometry-aware architecture that combines node features, Forman curvature summaries (LCP-style statistics), and Laplacian positional encodings (Dwivedi et al., 2022), followed by curvature-aware attention. Figure 1 provides an overview of ASEHybrid.

(E) Empirical validation and limitations Through controlled ablations on the CHAMELEON, SQUIRREL, TEXAS, TOLOKERS, and MINESWEEPER datasets, we show that geometry-aware GNNs yield large gains precisely when graph structure is label-informative, and offer negligible benefit otherwise. These results empirically validate our theoretical characterization of when geometric augmentation can improve over feature-only and position-only baselines, and complement prior work that identified label informativeness as a descriptive dataset property.

2. Background and Problem Setup

2.1. Graphs and Message-Passing GNNs

We consider node classification on an undirected simple graph $G = (V, E)$, where V is the set of nodes, $E \subseteq V \times V$

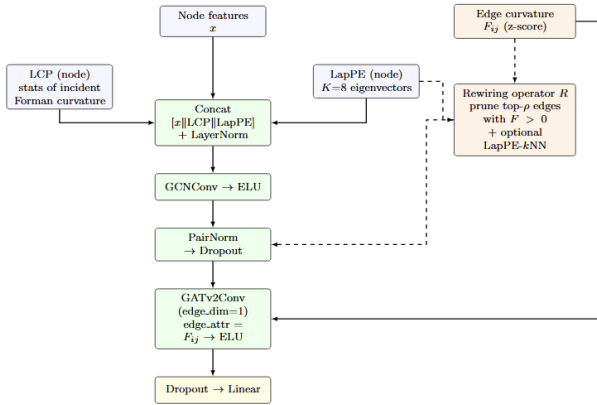


Figure 1. ASEHybrid overview. Node-side inputs (features x , LCP, LapPE) are concatenated and processed sequentially by GCNConv and curvature-conditioned GATv2 attention (edge_attr = F_{ij}), followed by a linear classifier. Curvature-guided rewiring R is a separate operator that edits the graph topology and is enabled only in rewiring-based variants (+Rewire and +Both).

the edge set, $x_v \in \mathbb{R}^d$ denotes the feature vector of node v , and $y_v \in \{1, \dots, C\}$ its class label. For a node $v \in V$, we write $\mathcal{N}(v)$ for its set of neighbors and $d_v := |\mathcal{N}(v)|$ for its degree. We use message-passing GNNs, where node representations are updated by aggregating information from neighboring nodes (formal definition in Appendix A.1). Standard message-passing GNNs are known to have limited expressive power; we revisit this issue in Section 4. In this work we focus on GATv2-style attention mechanisms. A standard GATv2 layer computes

$$h_v^{(\ell+1)} = \sigma \left(\sum_{u \in \mathcal{N}(v)} \alpha_{uv}^{(\ell)} W h_u^{(\ell)} \right),$$

where attention coefficients $\alpha_{uv}^{(\ell)}$ depend on the embeddings $h_u^{(\ell)}$ and $h_v^{(\ell)}$. In geometry-aware variants, the attention may additionally condition on a scalar edge attribute e_{uv} , yielding

$$\alpha_{uv}^{(\ell)} = \text{Attn} \left(h_u^{(\ell)}, h_v^{(\ell)}, e_{uv} \right).$$

This formulation will allow us to incorporate curvature-based edge signals while remaining within the message-passing framework.

2.2. Homophily, Adjusted Homophily, and Label Informativeness

A classical lens for analyzing GNN performance is *homophily*, the tendency of edges to connect nodes with the

same label. A commonly used edge homophily measure is

$$\begin{aligned} h_{\text{edge}} &:= \Pr(y_u = y_v \mid (u, v) \in E) \\ &= \frac{|\{(u, v) \in E : y_u = y_v\}|}{|E|}. \end{aligned}$$

However, raw homophily values are difficult to compare across datasets: they depend strongly on the number of classes and on class imbalance.

To address this issue, we adopt the *adjusted homophily* (assortativity) coefficient. Let

$$\bar{p}(k) := \frac{1}{2|E|} \sum_{v: y_v=k} d_v$$

denote the degree-weighted label distribution. The adjusted homophily is defined as

$$h_{\text{adj}} := \frac{h_{\text{edge}} - \sum_{k=1}^C \bar{p}(k)^2}{1 - \sum_{k=1}^C \bar{p}(k)^2}. \quad (1)$$

This quantity equals 1 for perfectly homophilous graphs, 0 for graphs whose edges are independent of labels under a configuration-model null, and is negative for systematically heterophilous graphs.

While adjusted homophily captures whether a graph is globally homo- or heterophilous, it does not directly quantify how informative neighborhoods are for prediction. To this end, we use *label informativeness* (LI). Let (ξ, η) be an ordered pair of endpoints of a uniformly sampled edge, and let y_ξ, y_η be their labels. Label informativeness is defined as the normalized mutual information

$$\text{LI} := \frac{I(y_\xi; y_\eta)}{H(y_\xi)} = \frac{H(y_\xi) - H(y_\xi \mid y_\eta)}{H(y_\xi)} \in [0, 1]. \quad (2)$$

LI equals 0 when neighbor labels are statistically independent and equals 1 when a neighbor's label uniquely determines the node's label. Empirically and theoretically, LI correlates much more strongly with GNN performance than homophily alone. In particular, there exist graphs that are heterophilous but informative (low h_{adj} and high LI), as well as heterophilous and uninformative (low h_{adj} and low LI).

In our framework, h_{adj} characterizes the global label structure, while LI quantifies the potential usefulness of local neighborhoods. ASEHybrid is designed to be sensitive to the latter: its geometric encodings and rewiring mechanisms aim to increase the *effective* label informativeness of the training graph.

2.3. When Can Graph Structure Help?

The distinction between homophily and label informativeness naturally leads to a more fundamental question: *when*

can access to graph structure improve prediction over feature-only models?

Let $X = (x_v)_{v \in V}$ denote node features, E the edge set, and $Y = (y_v)_{v \in V}$ the labels. In general, a baseline predictor may have access not only to X but also to additional node-level information that does not explicitly use E at test time (e.g., fixed positional encodings). We denote by \tilde{X} the total node-side information available to such a baseline (e.g., $\tilde{X} = X$ or $\tilde{X} = [X, \text{LapPE}]$).

We consider the conditional mutual information

$$I(Y; E \mid \tilde{X}),$$

which measures how much additional information about the labels is carried by the graph structure beyond what is already contained in \tilde{X} .

If $I(Y; E \mid \tilde{X}) = 0$, then the labels are conditionally independent of the edges given \tilde{X} , and access to graph structure cannot improve the Bayes-optimal prediction risk over predictors that only use \tilde{X} . Conversely, if $I(Y; E \mid \tilde{X}) > 0$, then there exist data distributions for which models that can exploit edge-derived signals achieve strictly lower risk than any predictor based only on \tilde{X} .

This information-theoretic criterion provides a unifying lens for the methods studied in this paper. Curvature-based encodings, positional geometry, and curvature-guided rewiring are useful only insofar as they extract or amplify label-relevant information from E that is not already present in \tilde{X} . We formalize this principle in Section 6.

3. Geometry-Aware Message Passing

3.1. Limitations of Laplacian Message Passing

Many popular GNN architectures, including GCNs and related models, implement message passing through variants of Laplacian smoothing. Repeated Laplacian-based propagation in GCN-style models admits a spectral characterization in the eigenbasis of the normalized Laplacian, where each component is scaled by a depth-dependent attenuation factor. A full derivation is provided in Appendix A.2.

3.2. Curvature-Weighted Diffusion

The formal definition of curvature-weighted diffusion and the corresponding message-passing update are provided in Appendix A.3.

Proposition 3.1 (Curvature-weighted diffusion reduces cross-class mixing). *Let $G = (V, E)$ be a graph with node labels $y : V \rightarrow \{1, \dots, C\}$. Define the baseline GCN transition kernel*

$$p_{ij} = \frac{w_{ij}}{\sum_k w_{ik}}, \quad w_{ij} := \frac{\mathbf{1}\{(i, j) \in E\}}{\sqrt{d_i d_j}},$$

and a curvature-weighted kernel

$$q_{ij} = \frac{w_{ij} s_{ij}}{\sum_k w_{ik} s_{ik}},$$

where $s_{ij} \geq 0$ is a curvature-dependent score.

Suppose that for each node i , if $J \sim p_i$. and we define

$$D := \mathbf{1}\{y_i \neq y_j\}, \quad S := s_{iJ},$$

then $\text{Cov}(S, D) \leq 0$. Then the expected cross-class mixing satisfies

$$\frac{1}{|V|} \sum_{i,j} q_{ij} \mathbf{1}\{y_i \neq y_j\} \leq \frac{1}{|V|} \sum_{i,j} p_{ij} \mathbf{1}\{y_i \neq y_j\}.$$

Proof. Deferred to Appendix B.1.

Lemma 3.2 (Sufficient condition via monotonicity). *If $S = f(U)$ for a non-increasing function f , and $\mathbb{E}[D \mid U]$ is non-decreasing in U , then $\text{Cov}(S, D) \leq 0$.*

Proof. Deferred to Appendix B.2.

3.3. Spectral Positional Geometry

Curvature captures local geometric structure but does not encode global positional information. To incorporate global geometry, we use Laplacian positional encodings (LapPE).

Let $L = I - \tilde{A}$ be the normalized Laplacian with eigenpairs (λ_k, ϕ_k) . Define the positional encoding matrix

$$P = [\phi_2, \dots, \phi_{K+1}] \in \mathbb{R}^{|V| \times K},$$

excluding the trivial constant eigenvector. Appending P to node features provides each node with coordinates in a global spectral embedding that are not smoothed by message passing.

Proposition 3.3 (Laplacian positional encodings mitigate spectral bias). *Let $\mathcal{H}_{\text{GCN}}^{(T)}$ denote the hypothesis class of a T -layer linearized GCN without positional encodings, and $\mathcal{H}_{\text{LapPE}}^{(T)}$ the corresponding class augmented with the first K nontrivial Laplacian eigenvectors. Then for any label signal y ,*

$$\min_{\hat{y} \in \mathcal{H}_{\text{LapPE}}^{(T)}} \|y - \hat{y}\|_2 \leq \|y - \Pi_{\text{span}(\phi_2, \dots, \phi_{K+1})} y\|_2,$$

provided $(1 - \lambda_k)^T \neq 0$ for all $k = 2, \dots, K + 1$.

Interpretation. The right-hand side of the inequality is the energy of the label signal y outside the span of the injected Laplacian eigenvectors. The proposition therefore states that a T -layer GCN augmented with Laplacian positional encodings can approximate y at least as well as its projection onto this spectral subspace. In particular, spectral components that would be attenuated by repeated Laplacian smoothing are preserved when supplied as positional inputs, provided they are not annihilated by propagation.

Proof. Deferred to Appendix 3.3.

Curvature-weighted diffusion and Laplacian positional encodings play complementary roles. Curvature reshapes local aggregation to suppress harmful mixing, while LapPE injects global, high-frequency structure that standard message passing cannot recover. Neither mechanism increases expressive power by itself; rather, they reshape information flow, a distinction formalized in the next section.

4. Expressivity of Geometry-Aware GNNs

In this section, we analyze the expressive power of geometry-aware message-passing GNNs. We distinguish between (i) local, degree-based geometric signals such as Forman curvature, (ii) non-local edge attributes derived from larger graph motifs, and (iii) positional encodings that provide global symmetry-breaking information. Our results clarify which forms of geometric augmentation can—and cannot—increase expressive power beyond the one-dimensional Weisfeiler–Lehman (1-WL) test.

4.1. No Expressivity Gain from Local Curvature

We first show that incorporating degree-based Forman curvature as an edge attribute does not increase the expressive power of message-passing GNNs.

Recall that the Forman curvature of an undirected edge (u, v) is

$$F(u, v) = 4 - \deg(u) - \deg(v),$$

which depends only on the degrees of its endpoints.

Theorem 4.1 (No WL gain from degree-based Forman curvature). *Any message-passing GNN that uses degree-based Forman curvature as an edge feature is no more expressive than the one-dimensional Weisfeiler–Lehman (1-WL) test.*

Proof. Deferred to Appendix B.4.

Implication. Local curvature does not act as a symmetry-breaking signal. Any empirical gains from curvature must therefore arise from improved information flow or stability, rather than increased representational capacity.

4.2. Gains from Non-Local Edge Attributes

We next contrast local curvature with non-local edge attributes that encode information beyond node degrees.

Theorem 4.2 (Expressivity gain with non-local edge attributes). *There exist pairs of non-isomorphic graphs that are indistinguishable by 1-WL, but can be distinguished by message-passing GNNs equipped with appropriate non-local, isomorphism-invariant edge attributes.*

Proof. Deferred to Appendix B.5.

4.3. Positional Encodings as Symmetry Breakers

We now turn to positional encodings, which provide nodes with global, graph-dependent coordinates.

Theorem 4.3 (PE-augmented expressivity gain). *There exist graph pairs that are indistinguishable by 1-WL, but can be distinguished with high probability by message-passing GNNs augmented with sufficiently rich positional encodings.*

Proof. Deferred to Appendix B.6.

Summary. Local curvature-based edge features do not increase expressive power beyond 1-WL, while non-local edge attributes and positional encodings can. This separation explains why curvature improves performance through improved diffusion and stability rather than symmetry breaking, and why combining curvature with positional geometry as in ASEHybrid is essential.

5. Curvature-Guided Rewiring

We study a curvature-guided rewiring process that modifies the graph structure during training. The goal is to remove edges that are geometrically redundant under a curvature-based score and to add edges that are consistent with global positional geometry (e.g., LapPE). We formalize the rewiring map and analyze its convergence and stability.

Rewiring operator. The rewiring procedure is formally defined in Appendix D.4.

5.1. Convergence of the Rewiring Dynamics

Proposition 5.1 (Finite termination of rewiring). *Suppose there exists a scalar objective $\mathcal{L}(E)$ such that $\mathcal{L}(E_{t+1}) < \mathcal{L}(E_t)$ whenever $E_{t+1} \neq E_t$. If the admissible edge sets form a finite space, then the rewiring process terminates after finitely many steps.*

Proof. Deferred to Appendix B.7.

5.2. Convergence and Local Stability of the Rewiring Map

We now show that, under eigengap and margin assumptions, the rewiring operator is locally constant around a fixed point.

Theorem 5.2 (Local stabilization of the rewiring map). *Let E^* be a fixed point of \mathcal{R} . Assume:*

1. **Eigengap.** *The normalized Laplacian of $G^* = (V, E^*)$ has an eigengap separating the retained LapPE subspace from the rest of the spectrum.*

2. ***kNN margin.*** For each node u , the k -th and $(k+1)$ -th nearest-neighbor distances in LapPE space are separated by a positive margin at E^* .

3. ***Pruning-score margin.*** Let $(e_1^*, \dots, e_{|E^*|}^*)$ be the ordering of $E^{*+} := \{e \in E^* : s^*(e) > 0\}$ by decreasing scores. Then

$$s^*(e_{\lceil \rho |E^{*+}| \rceil}^*) > s^*(e_{\lceil \rho |E^{*+}| \rceil + 1}^*)$$

(strict separation at the pruning threshold).

4. ***Score stability.*** The score map $E \mapsto s_E(\cdot)$ is continuous (or Lipschitz) in a neighborhood of E^* under bounded edge edits.

Then there exists a neighborhood \mathcal{U} of E^* such that for all $E \in \mathcal{U}$,

$$\mathcal{R}(E) = \mathcal{R}(E^*) = E^*.$$

In particular, \mathcal{R} is locally constant (and hence locally stable) at E^* .

Proof. Deferred to Appendix B.8.

5.3. Stability Under Edge Edits

We now bound how much the normalized adjacency changes under bounded edge edits, and propagate this to embedding stability.

Let $\tilde{A} := D^{-1/2}(A + I)D^{-1/2}$ denote the self-loop augmented normalized adjacency, and let $\tilde{d}_{\min} \geq 1$ denote the minimum degree after adding self-loops.

Lemma 5.3 (Operator-norm perturbation under edge edits). *Let E and E' be edge sets that differ by at most K edges. Let $\tilde{A}(E)$ and $\tilde{A}(E')$ denote the corresponding self-loop normalized adjacency matrices. Assume the degree ratio is bounded, i.e., $\tilde{d}_{\max}/\tilde{d}_{\min} \leq c$ for some constant c . Then*

$$\|\tilde{A}(E') - \tilde{A}(E)\|_2 \leq C \frac{K}{\tilde{d}_{\min}},$$

for a constant C depending only on c .

Proof. Deferred to Appendix B.9.

Corollary 5.4 (Lipschitz stability under bounded rewiring). *Consider a T -layer message-passing network with propagation operator $\tilde{A}(E)$ at each layer and weight matrices W_1, \dots, W_T . Assume the pointwise nonlinearity is 1-Lipschitz and $\tilde{d}_{\max}/\tilde{d}_{\min} \leq c$. If E and E' differ by at most K edges, then the output embeddings satisfy*

$$\|H_T(E') - H_T(E)\|_2 \leq C \frac{K}{\tilde{d}_{\min}} \prod_{\ell=1}^T \|W_\ell\|_2 \|H_0\|_2,$$

where C depends only on c .

Proof. Deferred to Appendix B.10.

Curvature-guided rewiring defines a discrete geometric flow over graphs. Under a strictly decreasing objective it terminates finitely, under eigengap and margin assumptions it stabilizes locally, and under bounded edge edits it induces controlled changes in normalized propagation and thus in embeddings.

6. When Does Geometry Help?

The preceding sections analyzed how curvature-based diffusion, positional geometry, and rewiring affect information flow and expressive power. We now address a more fundamental question: *when can access to graph structure improve prediction over models that do not explicitly use edges at test time?*

Our answer is information-theoretic. We show that the usefulness of geometry-aware GNNs is governed by whether graph structure carries label-relevant information beyond the information already available to the baseline predictor.

6.1. Edge-Label Information and Bayes Risk

Let $X = (x_v)_{v \in V}$ denote node features, E the edge set, and $Y = (y_v)_{v \in V}$ the node labels. In general, a baseline model may have access not only to X but also to additional node-level information that does not adapt to edges at test time (e.g., fixed positional encodings). We denote by \tilde{X} the total node-side information available to such a baseline.

We consider a probabilistic data-generating process over (\tilde{X}, E, Y) .

A \tilde{X} -only predictor is any measurable function $f : \tilde{X} \rightarrow \Delta(\mathcal{Y})$. An edge-aware predictor may additionally depend on E , $f : (\tilde{X}, E) \rightarrow \Delta(\mathcal{Y})$. Prediction quality is measured by expected risk under a proper scoring rule; for concreteness, we focus on log loss.

Under log loss, the Bayes-optimal risk of a predictor using information Z is

$$R^*(Z) = \mathbb{E}[-\log p(Y | Z)] = H(Y | Z),$$

the conditional entropy of Y given Z .

Consequently, the gap between the optimal \tilde{X} -only risk and the optimal edge-aware risk is

$$\begin{aligned} R^*(\tilde{X}) - R^*(\tilde{X}, E) &= H(Y | \tilde{X}) - H(Y | \tilde{X}, E) \\ &= I(Y; E | \tilde{X}), \end{aligned}$$

the conditional mutual information between labels and edges given \tilde{X} .

This quantity precisely measures the *potential benefit* of exploiting graph structure beyond the information already encoded in \tilde{X} .

6.2. Information-Theoretic Necessity and Sufficiency

We now state the main result of this section, which provides a sharp characterization of when geometry-aware methods can help.

Proposition 6.1 (Edge-label information governs usefulness). *Let (\tilde{X}, E, Y) be jointly distributed.*

1. (Necessity) *If $I(Y; E | \tilde{X}) = 0$, then no predictor that has access to E can achieve strictly lower Bayes risk than the optimal \tilde{X} -only predictor.*
2. (Sufficiency) *If $I(Y; E | \tilde{X}) > 0$, then there exists a data distribution and an edge-aware predictor that achieves strictly lower Bayes risk than any \tilde{X} -only predictor.*

Proof. Deferred to Appendix B.11.

Interpretation. Proposition 6.1 provides a complete characterization: geometry-aware methods are *provably useless* when edges add no label-relevant information beyond \tilde{X} , and *provably helpful* when they do.

When edge features or graph structure do not carry label-relevant information beyond node-side inputs, geometry-aware mechanisms cannot improve prediction in principle. In such regimes, feature-based or position-based models are sufficient, and incorporating edge-derived signals is unnecessary. This follows directly from the information-theoretic criterion governing when access to graph structure can reduce Bayes risk.

6.3. Implications for Geometry-Aware GNNs

A detailed discussion of these implications is provided in Appendix D.5.

7. Experiments

We evaluate *ASEHybrid* and controlled ablations thereof on five node-classification benchmarks selected to span a range of heterophilous regimes and label informativeness (LI) levels: **Chameleon** and **Squirrel** (Wikipedia web graphs; Section 7.1), **Texas** (WebKB citation network; Section 7.2), **Minesweeper** (high-baseline synthetic graph; Section 7.3), and **Tolokers** (large-scale crowdsourcing graph; Section 7.4). Following prior work, we use standard splits provided by PyTorch Geometric (Fey & Lenssen, 2019).¹

These datasets are chosen to test the central theoretical prediction of this paper: *geometry-aware mechanisms improve*

¹Chameleon/Squirrel: WikipediaNetwork (Rozemberczki et al., 2021); Texas: WebKB (Craven et al., 1998); Minesweeper/Tolokers: HeterophilousGraphDataset (Platonov et al., 2023).

performance precisely when graph structure carries label-relevant information beyond node-side features, and provide little or no benefit otherwise.

Architecture ASEHybrid combines curvature-augmented node features, curvature-aware attention, and optional curvature-guided rewiring. Full architectural details are provided in Appendix D.1.

Training. All models are trained under a common protocol with standard optimization and early stopping; full training details are provided in Appendix D.2.

Curvature-guided rewiring. Rewiring prunes a fraction $\rho \in \{0.01, 0.02\}$ of edges with the highest positive Forman curvature $F(i, j) = 4 - \deg(i) - \deg(j)$, and optionally adds $k \in \{0, 1\}$ k NN edges in Laplacian positional encoding (LapPE) space. Unless explicitly stated, rewiring is applied as a *one-shot preprocessing step*, consistent with the theoretical analysis of finite termination and local stability. Periodic rewiring is used only for ablation studies on small graphs.

Baselines and ablations. We compare against a vanilla two-layer GCN with ReLU activations, trained using the same splits and optimizer. Ablations are reported relative to **ASE base** and isolate the effects of (i) curvature-aware message passing and (ii) curvature-guided graph rewiring.

7.1. Ablations on Web Graphs

We begin with Chameleon and Squirrel, two canonical heterophilous web graphs known to exhibit high label informativeness despite low adjusted homophily. These datasets provide a setting where the theory predicts that access to graph structure should be strongly beneficial.

Rewiring yields the dominant performance gains (+16–17 points on Chameleon and +23–24 points on Squirrel; see Table 1), while curvature-aware message passing alone provides at most modest improvements. This behavior directly reflects the theoretical results: degree-based curvature does not increase expressive power beyond 1-WL, whereas curvature-guided rewiring can substantially improve information flow when edges are label-informative.

7.2. WebKB-Texas

Texas represents a smaller, moderately heterophilous graph with higher variance across splits and weaker global structural signal. Here, the theory predicts that geometry-aware methods may provide *consistent but modest* gains.

ASEHybrid achieves the highest mean accuracy across splits (see Table 1), with an absolute gain of +3.78 points over a

Table 1. Test accuracy (%) on heterophilous benchmarks (mean \pm std). Chameleon and Squirrel use fixed splits (10 seeds); Texas, Minesweeper, and Tolokers report results over dataset-provided splits. For Tolokers, curvature-guided rewiring is applied as a one-shot preprocessing step.

| METHOD | CHAMELEON | SQUIRREL | TEXAS | MINESWEEPER | TOLOKERS |
|--------------------------|------------------------------------|------------------------------------|------------------------------------|------------------------------------|------------------------------------|
| VANILLA GCN | 39.56 ± 2.32 | 28.29 ± 1.08 | 57.57 ± 6.12 | 80.04 ± 0.15 | 78.54 ± 0.33 |
| ASE BASE | 48.05 ± 1.47 | 32.08 ± 1.00 | 58.92 ± 5.06 | 80.06 ± 0.26 | 81.24 ± 0.47 |
| +EDGECURV | 48.05 ± 1.21 | 33.00 ± 0.73 | 58.11 ± 8.08 | 80.07 ± 0.17 | 81.28 ± 0.43 |
| +REWIRE | 64.47 ± 0.98 | 55.29 ± 0.70 | 59.19 ± 9.49 | 79.98 ± 0.34 | 80.32 ± 0.39 |
| +BOTH (ASEHYBRID) | 64.78 ± 0.77 | 56.13 ± 0.96 | 61.35 ± 6.87 | 80.05 ± 0.16 | 81.51 ± 0.43 |

vanilla GCN. While smaller than on the web graphs, the improvement is consistent with the information-theoretic criterion: edges in Texas carry limited but nonzero label-relevant information beyond node features, leading to modest but reliable gains.

7.3. Minesweeper: High-Baseline Regime

Results on the high-baseline Minesweeper benchmark are reported in Appendix D.3.

7.4. Tolokers: Large-Scale Graph

Tolokers is a large, noisy crowdsourcing graph with moderate label informativeness and substantial degree heterogeneity. Due to scale considerations, we apply curvature-guided rewiring as a single preprocessing step. ASEHybrid yields a consistent improvement over a vanilla GCN (see Table 1), while rewiring alone does not suffice. The modest gains observed here are consistent with theory: in large, heterogeneous graphs with noisy edges, geometry-aware mechanisms can improve stability and diffusion without producing dramatic performance jumps.

8. Related Work

Relation to prior work. Our work relates to prior studies on homophily and label informativeness, curvature-based graph learning, positional encodings, and graph rewiring. Unlike existing approaches, we provide a unified information-theoretic characterization of when graph structure can improve prediction, and establish formal convergence and stability guarantees for curvature-guided rewiring. A detailed discussion of related work is provided in Appendix C.

9. Conclusion

We studied geometry-aware graph neural networks through a unified theoretical and empirical lens, clarifying the roles of homophily, label informativeness, curvature, positional encodings, and graph rewiring in heterophilous node classification.

On the theory side, we showed that local, degree-based geometric signals such as Forman curvature do not increase expressive power beyond the one-dimensional Weisfeiler–Lehman test, but can substantially improve performance by reshaping diffusion and reducing harmful cross-class mixing. In contrast, non-local edge attributes and positional encodings can strictly increase expressive power by breaking graph symmetries. For curvature-guided rewiring, we established finite termination, local stabilization, and Lipschitz stability under bounded edge edits.

These results lead to a sharp information-theoretic characterization of when geometry helps: geometry-aware mechanisms are useful precisely when graph structure carries label-relevant information beyond node features, as measured by conditional edge–label mutual information. Our experiments corroborate this prediction, showing large gains on label-informative heterophilous graphs, modest improvements on smaller benchmarks, and comparable performance when node features alone are already highly predictive.

We instantiated these insights in *ASEHybrid*, a practical geometry-aware architecture that consistently outperforms vanilla message passing across diverse heterophilous benchmarks while remaining computationally efficient.

Impact Statement

This paper advances the theoretical understanding and design of geometry-aware graph neural networks. The methods studied operate on abstract graph structures and are agnostic to the semantic content of node features or labels, and therefore do not introduce new sources of bias beyond those present in the underlying data. While graph-based models may be applied in sensitive domains, any broader societal or ethical impacts depend on downstream use and deployment, which are beyond the scope of this work.

References

Brody, S., Alon, U., and Yahav, E. How attentive are graph attention networks? In *ICLR*, 2022.

Craven, M., DiPasquo, D., Freitag, D., McCallum, A., Mitchell, T., Nigam, K., and Slattery, S. Learning to

extract symbolic knowledge from the world wide web. In *Proceedings of the Fifteenth National Conference on Artificial Intelligence (AAAI)*, 1998.

Dwivedi, V. P. and Bresson, X. A generalization of transformer networks to graphs. *arXiv preprint arXiv:2012.09699*, 2020.

Dwivedi, V. P., Luu, A. T., Laurent, T., Bengio, Y., and Bresson, X. Graph neural networks with learnable structural and positional representations. In *International Conference on Learning Representations (ICLR)*, 2022.

Fesser, L. and Weber, M. Effective structural encodings via local curvature profiles. In *The Twelfth International Conference on Learning Representations (ICLR)*, 2024.

Fey, M. and Lenssen, J. E. Fast graph representation learning with pytorch geometric. *arXiv preprint arXiv:1903.02428*, 2019.

Forman. Bochner's method for cell complexes and combinatorial ricci curvature. *Discrete & Computational Geometry*, 29(3):323–374, 2003.

Gilmer, J., Schoenholz, S. S., Riley, P. F., Vinyals, O., and Dahl, G. E. Neural message passing for quantum chemistry. In *International conference on machine learning*, pp. 1263–1272. Pmlr, 2017.

Kipf, T. N. and Welling, M. Semi-supervised classification with graph convolutional networks. In *International Conference on Learning Representations (ICLR)*, 2017.

Ma, Y., Liu, X., Shah, N., and Tang, J. Is homophily a necessity for graph neural networks? In *International Conference on Learning Representations (ICLR)*, 2022.

Ollivier, Y. Ricci curvature of markov chains on metric spaces. *Journal of Functional Analysis*, 256(3):810–864, 2009.

Oono, K. and Suzuki, T. Graph neural networks exponentially lose expressive power for node classification. In *International Conference on Learning Representations (ICLR)*, 2020.

Platonov, O., Kuznedelev, D., Babenko, A., and Prokhorenkova, L. Characterizing graph datasets for node classification: Homophily-heterophily dichotomy and beyond. *Advances in Neural Information Processing Systems*, 36:523–548, 2023.

Rozemberczki, B., Allen, C., and Sarkar, R. Multi-scale attributed node embedding. *Journal of Complex Networks*, 9(2):cnab014, 2021.

Sato, R., Yamada, M., and Kashima, H. Random features strengthen graph neural networks. In *Proceedings of the 2021 SIAM international conference on data mining (SDM)*, pp. 333–341. SIAM, 2021.

Scarselli, F., Gori, M., Tsoi, A. C., Hagenbuchner, M., and Monfardini, G. The graph neural network model. *IEEE transactions on neural networks*, 20(1):61–80, 2008.

Sreejith, R. P., Mohanraj, K., Jost, J., Saucan, E., and Samal, A. Forman curvature for complex networks. *Journal of Statistical Mechanics: Theory and Experiment*, 2016(6):063206, 2016.

Topping, J. et al. Understanding over-squashing and bottlenecks on graphs via curvature. In *ICLR*, 2022.

Xu, K., Hu, W., Leskovec, J., and Jegelka, S. How powerful are graph neural networks? In *International Conference on Learning Representations (ICLR)*, 2019.

Zhao, L. and Akoglu, L. Pairnorm: Tackling oversmoothing in gnns. In *ICLR*, 2020.

Zhu, J., Yan, Y., Zhao, L., Heimann, M., Akoglu, L., and Koutra, D. Beyond homophily in graph neural networks: Current limitations and effective designs. *Advances in neural information processing systems*, 33:7793–7804, 2020.

1. (A) Notation

Table 2 summarizes the main notation used throughout the paper.

Table 2. Summary of notation used throughout the paper.

| Symbol | Description |
|--------------------------------------|--|
| $G = (V, E)$ | Undirected graph with node set V and edge set E |
| $n = V $ | Number of nodes |
| $m = E $ | Number of edges |
| v, u, i, j | Node indices |
| $\mathcal{N}(v)$ | Neighborhood of node v |
| d_v | Degree of node v |
| A | Adjacency matrix of G |
| D | Diagonal degree matrix |
| \tilde{A} | Normalized adjacency $D^{-1/2}(A + I)D^{-1/2}$ |
| L | Normalized graph Laplacian $I - \tilde{A}$ |
| λ_k, ϕ_k | k -th eigenvalue and eigenvector of L |
| T | Number of message-passing layers / propagation steps |
| K | Number of Laplacian positional encoding dimensions |
| P | Laplacian positional encoding matrix $[\phi_2, \dots, \phi_{K+1}]$ |
| $x_v \in \mathbb{R}^d$ | Input feature vector of node v |
| X | Matrix of node features $(x_v)_{v \in V}$ |
| \tilde{X} | Node-side information available to feature-only or PE-only baselines |
| $y_v \in \{1, \dots, C\}$ | Class label of node v |
| Y | Vector of node labels $(y_v)_{v \in V}$ |
| $h_v^{(\ell)}$ | Node representation of v at layer ℓ |
| $H^{(\ell)}$ | Matrix of node representations at layer ℓ |
| $W^{(\ell)}$ | Trainable weight matrix at layer ℓ |
| $\sigma(\cdot)$ | Pointwise nonlinearity |
| AGG | Permutation-invariant aggregation operator |
| e_{uv} | Edge attribute associated with edge (u, v) |
| F_{uv} | Degree-based Forman curvature of edge (u, v) |
| $f(\cdot)$ | Curvature-based edge weighting function |
| p_{ij} | Baseline GCN transition kernel |
| q_{ij} | Curvature-weighted transition kernel |
| s_{ij} | Curvature-dependent edge score |
| h_{edge} | Edge homophily |
| h_{adj} | Adjusted homophily (assortativity) |
| LI | Label informativeness |
| $I(\cdot; \cdot)$ | Mutual information |
| $I(\cdot; \cdot \cdot)$ | Conditional mutual information |
| $R^*(Z)$ | Bayes-optimal risk given information Z |
| R | Curvature-guided rewiring operator |
| $G_t = (V, E_t)$ | Graph at rewiring step t |
| E_t | Edge set at rewiring step t |
| ρ | Fraction of edges pruned during rewiring |
| k | Number of nearest neighbors added in LapPE space |
| $\tilde{d}_{\min}, \tilde{d}_{\max}$ | Minimum / maximum degree after self-loop augmentation |

A. Additional Background

A.1. Message-Passing GNNs and Expressivity

A generic message-passing graph neural network (GNN) updates node representations according to

$$h_v^{(\ell+1)} = \sigma \left(\text{AGG} \left\{ \phi \left(h_v^{(\ell)}, h_u^{(\ell)}, e_{uv} \right) : u \in \mathcal{N}(v) \right\} \right),$$

where $h_v^{(\ell)}$ is the representation of node v at layer ℓ , e_{uv} is an optional edge feature, ϕ is a learnable message function, AGG is a permutation-invariant aggregation operator, and σ is a nonlinearity. It is well known that such message-passing architectures are limited in expressive power: when initialized from the same node features, they are at most as powerful as

the one-dimensional Weisfeiler–Lehman (1-WL) test for distinguishing non-isomorphic graphs. This limitation applies even when edge features are present, provided these features are functions of local graph structure and do not encode non-local or positional information.

A.2. Spectral View of Laplacian Message Passing

Let A denote the adjacency matrix of G , D the diagonal degree matrix, and $\tilde{A} = D^{-1/2}(A + I)D^{-1/2}$ the normalized adjacency. A linearized GCN layer takes the form

$$H^{(\ell+1)} = \tilde{A}H^{(\ell)}W.$$

Let $L = I - \tilde{A}$ denote the normalized Laplacian, with eigendecomposition $L = \Phi\Lambda\Phi^\top$, where $0 = \lambda_1 \leq \lambda_2 \leq \dots \leq \lambda_n \leq 2$. Repeated propagation yields

$$H^{(T)} = \tilde{A}^TH^{(0)}W^{(T)} = \Phi(I - \Lambda)^T\Phi^\top H^{(0)}W^{(T)}.$$

Thus, each eigenmode ϕ_k is scaled by $(1 - \lambda_k)^T$, where T is the number of propagation steps (layers) in the linearized model. Since $I - \Lambda$ is diagonal, $(I - \Lambda)^T$ raises each diagonal entry $(1 - \lambda_k)$ to the T -th power. High-frequency components (large λ_k) are exponentially attenuated, while low-frequency components dominate. This induces a strong low-pass bias, favoring label signals that vary smoothly over edges (Oono & Suzuki, 2020).

In heterophilous graphs, class labels often exhibit significant high-frequency energy. As a result, Laplacian smoothing mixes features across class boundaries, leading to over-smoothing and degraded performance. This motivates geometry-aware modifications that selectively attenuate harmful aggregation without abandoning message passing entirely.

A.3. Curvature-Weighted Diffusion (Definition and Update Rule)

To modulate message passing based on local graph geometry, we introduce a degree-based Forman curvature for undirected edges. For an undirected edge $(i, j) \in E$, we define the (degree-based) Forman curvature

$$F_{ij} := 4 - d_i - d_j,$$

where $d_i := |\mathcal{N}(i)|$ denotes the degree of node i (Forman, 2003). Edges connecting high-degree nodes or structurally inconsistent regions tend to have large negative curvature, while edges inside cohesive neighborhoods exhibit higher curvature.

In geometry-aware message passing, curvature enters as a scalar edge attribute that conditions aggregation weights. A curvature-weighted diffusion step takes the form

$$h_i^{(\ell+1)} = \sigma \left(\sum_{j \in \mathcal{N}(i)} f(F_{ij}) \frac{1}{\sqrt{d_i d_j}} W h_j^{(\ell)} \right),$$

where $f : \mathbb{R} \rightarrow \mathbb{R}_{\geq 0}$ is a monotone or learnable weighting function, typically implemented via attention.

This formulation corresponds to anisotropic diffusion: aggregation across low-curvature edges is attenuated relative to standard Laplacian smoothing.

We now formalize the intuition that curvature-based reweighting reduces cross-class mixing.

B. Additional Proofs

B.1. Proof of Proposition 3.1

Proof. Fix a node i . Sampling $J \sim q_i$ corresponds to sampling $J \sim p_i$ under importance weighting by the nonnegative scores $S = s_{iJ}$. In particular, for any function φ ,

$$\mathbb{E}_q[\varphi(J)] = \frac{\mathbb{E}_p[\varphi(J)S]}{\mathbb{E}_p[S]}.$$

Applying this identity with $\varphi(J) = D$ yields

$$\mathbb{E}_q[D] = \frac{\mathbb{E}_p[DS]}{\mathbb{E}_p[S]}.$$

Since $\text{Cov}(S, D) \leq 0$, we have $\mathbb{E}_p[DS] \leq \mathbb{E}_p[D]\mathbb{E}_p[S]$. Substituting gives $\mathbb{E}_q[D] \leq \mathbb{E}_p[D]$. Averaging over all nodes $i \in V$ yields the stated inequality. \square

The covariance condition admits a natural sufficient condition.

B.2. Proof of Lemma 3.2

Proof. Let U' be an independent copy of U , and let D' be the corresponding copy of D . Using the identity

$$\text{Cov}(f(U), D) = \frac{1}{2} \mathbb{E}[(f(U) - f(U'))(D - D')],$$

we examine the sign of the integrand. Since f is non-increasing and $\mathbb{E}[D \mid U]$ is non-decreasing, $(f(U) - f(U'))(D - D') \leq 0$ almost surely. Taking expectations yields $\text{Cov}(S, D) \leq 0$. \square

B.3. Proof of Proposition 3.3

Proof. Let $L = \Phi\Lambda\Phi^\top$ be the normalized Laplacian eigendecomposition. Repeated propagation yields

$$\tilde{A}^T = \Phi(I - \Lambda)^T\Phi^\top.$$

On the subspace $\text{span}(\phi_2, \dots, \phi_{K+1})$, the operator \tilde{A}^T is invertible under the stated condition. Thus any signal in this subspace can be exactly represented by propagating the positional encodings, and the best approximation error over $\mathcal{H}_{\text{LapPE}}^{(T)}$ is bounded by the projection residual. \square

B.4. Proof of Theorem 4.1

Proof. We prove the claim by a simulation argument.

Let G and G' be two graphs that are indistinguishable by 1-WL. By definition, there exists a sequence of bijections $\phi_t : V(G) \rightarrow V(G')$ preserving node colors at every WL iteration.

After the first WL iteration, the color of each node uniquely determines its degree. Thus, degrees are 1-WL-definable. Since the Forman curvature $F(u, v)$ is a deterministic function of $\deg(u)$ and $\deg(v)$, the multiset of curvature values on edges incident to a node is also preserved under ϕ_t .

Consider a message-passing GNN that conditions aggregation on $F(u, v)$. At each layer, the updated node representation is a function of the multiset of neighbor representations and curvature values. Because both node degrees and curvature values are invariant under the WL bijections ϕ_t , the entire message-passing update can be simulated by a 1-WL refinement started from the same initial node labels.

Formally, this follows from the fact that initializing 1-WL with labels that are deterministic functions of previous WL colors does not increase its distinguishing power. Therefore, curvature-augmented message passing cannot distinguish any pair of graphs that 1-WL fails to distinguish, and does not increase expressive power beyond 1-WL. \square

B.5. Proof of Theorem 4.2

Proof. Consider two d -regular graphs G_1 and G_2 on the same number of nodes, where G_1 is triangle-free and G_2 contains at least one triangle. Such graphs are indistinguishable by 1-WL.

Define an edge attribute

$$e(u, v) := |\mathcal{N}(u) \cap \mathcal{N}(v)|,$$

the number of common neighbors of u and v . This attribute is invariant under graph isomorphisms but is not determined by node degrees alone.

In G_1 , all edges satisfy $e(u, v) = 0$, whereas in G_2 , edges participating in triangles satisfy $e(u, v) > 0$. An edge-labeled 1-WL refinement distinguishes these graphs after one iteration, and a message-passing GNN that conditions aggregation on $e(u, v)$ can simulate this refinement.

Hence, non-local edge attributes can strictly increase expressive power beyond 1-WL. \square

B.6. Proof of Theorem 4.3

Proof. Let G be a graph with nontrivial automorphisms, such that 1-WL assigns the same color to all nodes. Assign to each node v a positional encoding $p_v \in \mathbb{R}^k$ such that

$$\sum_{u \in S} p_u \neq \sum_{u \in T} p_u \quad \text{for all distinct multisets } S \neq T.$$

This condition holds with probability one if the p_v are drawn from a continuous distribution, or when Laplacian eigenvectors are in general position (i.e., do not satisfy accidental linear dependencies).

Define

$$s(v) := \sum_{u \in \mathcal{N}(v)} p_u.$$

Under the stated condition, the mapping $v \mapsto (p_v, s(v))$ uniquely determines the neighborhood multiset of v . A single message-passing layer can compute $s(v)$, and an MLP can map $(p_v, s(v))$ to unique node representations.

Thus, the GNN distinguishes nodes and hence graphs that 1-WL cannot distinguish \square

B.7. Proof of Proposition 5.1

Proof. Since V is fixed, the space of admissible edge sets is finite. If $\mathcal{L}(E)$ strictly decreases whenever rewiring changes the edge set, then the sequence $\{\mathcal{L}(E_t)\}$ is strictly decreasing and cannot cycle. Hence the process must reach a fixed point E^* after finitely many steps, i.e., $E_{t+1} = E_t = E^*$. \square

B.8. Proof of Theorem 5.2

Proof. We show that both the added-edge set and the pruned-edge set are locally unchanged near E^* .

(LapPE stability). Perturbations of the normalized Laplacian in operator norm induce perturbations of the Laplacian eigenvectors of order $O(\|\Delta L\|/\text{gap})$ on the retained subspace. Under the eigengap assumption, LapPE vary continuously (indeed Lipschitz) for E close enough to E^* .

(Stability of k NN additions). By the k NN margin assumption, sufficiently small perturbations of LapPE do not change each node's set of k nearest neighbors. Hence the set of added edges is identical to that at E^* for all E in a small neighborhood.

(Stability of pruning). By the pruning-score margin and the score stability assumption, the ordering of positive-curvature edge scores near the pruning threshold is unchanged for all E close enough to E^* . Therefore, the top $\lceil \rho |E^+| \rceil$ edges selected for removal are the same as at E^* .

Combining these two facts, the rewiring step performs exactly the same edge deletions and additions as at E^* , implying $\mathcal{R}(E) = \mathcal{R}(E^*) = E^*$. \square

B.9. Proof of Lemma 5.3

Proof. Consider a single edge insertion or deletion. Let A' and D' denote the resulting adjacency and degree matrices. We write

$$\begin{aligned} \tilde{A}(E') - \tilde{A}(E) &= (D'^{-1/2} - D^{-1/2})(A + I)D^{-1/2} \\ &\quad + D'^{-1/2}(A' - A)D^{-1/2} \\ &\quad + D'^{-1/2}(A' + I)(D'^{-1/2} - D^{-1/2}). \end{aligned} \tag{3}$$

The adjacency difference $A' - A$ is a rank-two matrix with operator norm at most 1, and the (self-loop augmented) degree of any node changes by at most 1. For diagonal degree matrices, applying the mean value theorem to $f(x) = x^{-1/2}$ yields

$$\|D'^{-1/2} - D^{-1/2}\|_2 \leq \frac{1}{2\tilde{d}_{\min}^{3/2}}.$$

Moreover, using the factorization $(A + I)D^{-1/2} = D^{1/2}\tilde{A}(E)$, we obtain

$$\|(A + I)D^{-1/2}\|_2 \leq \sqrt{\tilde{d}_{\max}} \|\tilde{A}(E)\|_2 \leq \sqrt{\tilde{d}_{\max}},$$

where $\|\tilde{A}(E)\|_2 \leq 1$ for the normalized operator. Under the bounded degree ratio assumption, $\sqrt{\tilde{d}_{\max}} \leq \sqrt{c\tilde{d}_{\min}}$.

Using submultiplicativity of the operator norm and $\|D^{-1/2}\|_2, \|D'^{-1/2}\|_2 \leq 1/\sqrt{\tilde{d}_{\min}}$, we obtain

$$\|D'^{-1/2}(A' - A)D^{-1/2}\|_2 \leq \frac{1}{\tilde{d}_{\min}},$$

and

$$\|(D'^{-1/2} - D^{-1/2})(A + I)D^{-1/2}\|_2 \leq \frac{\sqrt{c}}{2\tilde{d}_{\min}}.$$

The third term in (3) is bounded analogously. Hence, a single edge edit perturbs \tilde{A} by at most C/\tilde{d}_{\min} for a constant C depending only on c . By subadditivity of the operator norm, K such edits yield

$$\|\tilde{A}(E') - \tilde{A}(E)\|_2 \leq C \frac{K}{\tilde{d}_{\min}}.$$

□

B.10. Proof of Corollary 5.4

Proof. By Lemma 5.3, $\|\tilde{A}(E') - \tilde{A}(E)\|_2 \leq CK/\tilde{d}_{\min}$. Each layer map is Lipschitz with constant at most $\|\tilde{A}(E)\|_2\|W_\ell\|_2$, and $\|\tilde{A}(E)\|_2 \leq 1$ for the normalized operator. Composing the perturbation through T layers yields the stated bound. □

B.11. Proof of Proposition 6.1

Proof. We prove the two parts separately.

Necessity. If $I(Y; E | \tilde{X}) = 0$, then Y and E are conditionally independent given \tilde{X} . Hence

$$p(Y | \tilde{X}, E) = p(Y | \tilde{X}) \quad \text{a.s.}$$

The Bayes-optimal predictor using (\tilde{X}, E) therefore coincides with the Bayes-optimal predictor using \tilde{X} alone, implying

$$R^*(\tilde{X}, E) = R^*(\tilde{X}).$$

Sufficiency. If $I(Y; E | \tilde{X}) > 0$, then

$$H(Y | \tilde{X}, E) < H(Y | \tilde{X}),$$

so the Bayes-optimal edge-aware predictor achieves strictly lower risk than the Bayes-optimal \tilde{X} -only predictor. □

C. Related Work

Homophily, heterophily, and label informativeness. The effectiveness of message-passing GNNs has traditionally been explained through *homophily*, the tendency of neighboring nodes to share labels (Kipf & Welling, 2017). However, recent work has shown that homophily alone is insufficient: graphs with similar homophily levels can exhibit vastly different GNN behavior, and some heterophilous graphs remain amenable to standard message passing (Zhu et al., 2020; Ma et al., 2022). To address this limitation, adjusted homophily (assortativity) and *label informativeness* (LI) were proposed as more principled descriptors of graph structure (Platonov et al., 2023). LI measures how informative a neighbor's label is about a node's label and has been shown to correlate more strongly with GNN performance than raw homophily. Our work builds on this line of research by providing an information-theoretic criterion for when graph structure can improve prediction, and by analyzing how geometric mechanisms interact with label informativeness.

Curvature and structural encodings. Discrete Ricci curvature notions, including Forman and Ollivier curvature, have been used to characterize local graph geometry (Forman, 2003; Ollivier, 2009; Sreejith et al., 2016). Recent work introduced curvature-based structural encodings and local curvature profiles as node features for GNNs, reporting empirical gains especially on heterophilous benchmarks (Fesser & Weber, 2024). These methods are typically motivated heuristically. In contrast, we show that degree-based Forman curvature does not increase expressivity beyond 1-WL, but can improve performance by reshaping diffusion and reducing harmful cross-class mixing.

Positional encodings. Positional encodings have been widely studied as a means of injecting global structure into GNNs (Dwivedi & Bresson, 2020; Dwivedi et al., 2022). Laplacian eigenvectors and related spectral features have been shown to mitigate over-smoothing and to increase expressive power by breaking graph symmetries. Our analysis complements this work by formalizing how Laplacian positional encodings counteract the low-pass bias of Laplacian smoothing and interact with geometry-aware message passing.

Graph rewiring. Graph rewiring and topology augmentation have been proposed to alleviate information flow bottlenecks such as over-squashing in deep GNNs (Topping et al., 2022). Existing approaches include heuristic edge pruning, curvature-guided rewiring, and learned topology modification. Although effective in practice, most rewiring methods come with limited algorithmic guarantees. We contribute to this literature by analyzing a simple curvature-guided rewiring process, establishing finite termination, local stabilization, and Lipschitz stability under bounded edge edits.

Expressivity of GNNs. The expressive power of message-passing GNNs is known to be bounded by the one-dimensional Weisfeiler–Lehman (1-WL) test (Xu et al., 2019). Recent work has shown that augmenting GNNs with random node features can enable them to distinguish some graphs that 1-WL cannot (Sato et al., 2021). Our results refine this understanding by separating local, degree-based geometric signals from non-local edge attributes and positional encodings, and by identifying which geometric augmentations can and cannot exceed the 1-WL expressivity ceiling.

Unlike prior work that studies curvature, positional encodings, or rewiring in isolation, we present a unified theoretical framework that connects these mechanisms through label informativeness and conditional edge–label information, clarifying when geometry-aware GNNs should be expected to help.

D. Experimental Details

D.1. Architecture

ASE base is a geometry-augmented but *static* model that concatenates raw node features with local curvature profiles (LCP) and Laplacian positional encodings (LapPE), without modifying graph structure or using edge-level curvature during message passing. **ASEHybrid** extends ASE base by incorporating curvature-aware attention and optional curvature-guided rewiring.

Concretely, ASEHybrid follows the pipeline: LayerNorm → GCNConv → ELU → PairNorm (Zhao & Akoglu, 2020) → GATv2 (Brody et al., 2022) (`edge_dim = 1`) → Linear. Input features concatenate raw node attributes with LCP (five statistics: min/max/mean/std/median of incident Forman curvatures) and Laplacian positional encodings (LapPE; $K = 8$ eigenvectors) (Sato et al., 2021). All graphs are symmetrized, self-loops removed, and edges coalesced.

D.2. Training Protocol

All models are trained using AdamW (learning rate 0.003–0.005 for ASEHybrid, 0.01 for GCN; weight decay 5×10^{-4}), for 700–800 epochs with early stopping (patience 120–150). Unless stated otherwise, results are reported as mean \pm standard deviation over **10 random seeds** for datasets with a fixed split (Chameleon, Squirrel), and over the **dataset-provided splits** (10 in PyTorch Geometric) for WebKB–Texas and HeterophilousGraphDataset benchmarks (Minesweeper, Tolokers).

D.3. Minesweeper: High-Baseline Regime

Minesweeper is a synthetic benchmark where node features alone are highly predictive and label informativeness of edges is minimal. The theory predicts that geometry-aware mechanisms should not improve performance in this regime.

As expected, all methods perform nearly identically (see Table 1). This serves as a necessary sanity check, empirically confirming the theoretical claim that when $I(Y; E \mid \tilde{X}) = 0$, no geometric augmentation can improve Bayes-optimal

prediction.

D.4. Curvature-Guided Rewiring Algorithm

Let $G_t = (V, E_t)$ denote the graph at rewiring step t , with $m_t := |E_t|$. Given node representations (or positional encodings) and associated geometric signals, a single rewiring step applies:

1. **Score and prune edges.** Each edge $(u, v) \in E_t$ is assigned a score $s_t(u, v)$; in our instantiation, $s_t(u, v)$ is the Forman curvature of the edge computed on G_t .

Pruning is restricted to edges with *positive* score, which we denote by

$$E_t^+ := \{e \in E_t : s_t(e) > 0\}.$$

Let $(e_1, \dots, e_{|E_t^+|})$ be an ordering of E_t^+ such that

$$s_t(e_1) \geq s_t(e_2) \geq \dots \geq s_t(e_{|E_t^+|}).$$

For a fixed $\rho \in (0, 1)$, remove the top $\lceil \rho |E_t^+| \rceil$ edges $\{e_1, \dots, e_{\lceil \rho |E_t^+| \rceil}\}$. If $E_t^+ = \emptyset$, no edges are pruned.

2. **Add k NN edges in LapPE space.** Compute Laplacian positional encodings $P_t = [\phi_2, \dots, \phi_{K+1}]$ on G_t . For each node u , add edges to its k nearest neighbors under the Euclidean metric in LapPE space (excluding existing neighbors and u itself).
3. **Update.** Recompute the geometric scores on the updated graph to obtain G_{t+1} .

This defines a (possibly stochastic) rewiring operator

$$\mathcal{R} : E_t \mapsto E_{t+1}.$$

D.5. Implications for Geometry-Aware GNNs

Why curvature and rewiring help. Curvature-based encodings and rewiring modify how information from E is propagated and emphasized. When $I(Y; E \mid \tilde{X}) > 0$, these mechanisms can amplify informative edges and suppress misleading ones, effectively increasing the usable signal extracted from the graph.

Why geometry sometimes fails. When $I(Y; E \mid \tilde{X}) = 0$, no manipulation of E —including curvature weighting, positional encodings derived from E , or rewiring can improve prediction in principle. In such regimes, empirical gains are not expected, and \tilde{X} -only baselines are optimal.

Relation to label informativeness. Label informativeness (LI) measures mutual information between labels at the endpoints of a random edge. While LI is not identical to $I(Y; E \mid \tilde{X})$, it provides a practical proxy: high LI suggests that edges are informative about labels, whereas low LI indicates that edges are uninformative given node-side information. Our theory (Proposition 6.1) explains why geometry-aware GNNs tend to succeed precisely on datasets with high LI.

Summary. The usefulness of geometry-aware message passing is not determined by homophily alone, nor by architectural sophistication. Rather, it is fundamentally governed by whether graph structure contains label-relevant information beyond the node-side information \tilde{X} already available to the predictor.